

Received May 5, 2018, accepted June 1, 2018, date of publication June 29, 2018, date of current version July 19, 2018.

Digital Object Identifier 10.1109/ACCESS.2018.2850743

# Unscented Kalman Filter-Based Battery SOC Estimation and Peak Power Prediction Method for Power Distribution of Hybrid Electric Vehicles

WEIDA WANG, XIANTAO WANG<sup>ID</sup>, CHANGLE XIANG, CHAO WEI, AND YULONG ZHAO

School of Mechanical Engineering, Beijing Institute of Technology, Beijing 100081, China

Corresponding author: Weida Wang (wangwd0430@163.com)

This work was supported by the National Natural Science Foundation of China under Grants 51575043 and U1564210.

**ABSTRACT** State of Charge (SOC) is a key parameter for battery management and vehicle energy management. Recently used SOC estimation methods for lithium-ion battery for vehicles have problems of too simple a base model for the battery and large sampling noise in both the voltage and current signals. To improve the accuracy of SOC estimation and consider that the extended Kalman filter algorithm needs linear approximation of the system equation, the unscented Kalman filter (UKF) algorithm was used to reduce the influence of sampling noise, and an improved algorithm with better filtering effect and SOC estimation accuracy was proposed. Based on the SOC estimation and battery model, the peak power prediction method for the battery is proposed and used in the power distribution strategy for Series HEV. Considering the frequent changes in load current and sampling noise, an experiment was designed to verify the effectiveness and robustness of the algorithm. The experimental results show that the UKF algorithm and the improved UKF algorithm can achieve 6% and 1.5% estimation error. The power distribution strategy based on battery SOC estimation and peak power prediction is tested and validated.

**INDEX TERMS** Lithium-ion battery, SOC estimation, unscented Kalman filter, noise suppression, peak power prediction.

## I. INTRODUCTION

Following popular demand, the development of technology and government support, new energy vehicles have become more popular. Lithium-ion batteries have the advantage of large capacity, and high power, and are usually used in new-energy vehicles [1]. A lithium-ion battery is one of the core components of an Hybrid Electric Vehicle(HEV), it is a complex chemical system, and needs BMS for its precise management [2]. SOC is one of the key links in the vehicle energy management chain, and provides the basis for the remaining range forecast [3]. Due to the internal state of the battery not being measurable, estimation of battery SOC is a difficult problem. The external voltage and current can be measured but are always contaminated by noise, so the Kalman filter method can be used to iterate from the noise signal to estimate the SOC of the battery [4], [5].

Common SOC estimation methods usually include ampere-hour integral method, open circuit voltage method, neural network intelligent algorithms, and so on [6].

The former two methods, because of the needs of accurate initial SOC value and high measurement accuracy [7], [8], could not be applied directly in dynamic conditions. A large experimental dataset is used to train the neural network model, and its actual performance is not good. The Kalman filter method based on the battery state space equation has strong applicability and versatility [9], which overcomes the problems of the need of the initial SOC value of the battery, and the large number of experimental data points for training [10]. Meanwhile, its filtering principle can significantly reduce the influence of sampling noise [11]. Due to the non-linear characteristics of the battery, EKF and UKF algorithms are used in the battery estimation algorithm. Some studies have proved that the UKF algorithm has better accuracy. This is due to the fact that the EKF algorithm takes the first order approximation of the system equation and only achieves first order accuracy [12]–[14], but the UKF algorithm uses pre-determined sampling points to sample the system, and the theoretical analysis has proved that it can achieve second order accuracy [11].

In the UKF algorithm application, there are the following issues: it can reduce the effect of noise to a certain extent, but too much measurement noise still has a significant effect on the implementation of the algorithm, and even causes divergence. Due to influence of external factors, the sampling data beyond the normal range in one or several sampling periods will make the SOC estimation algorithm generate significant error, and the convergence speed decreases.

One of the bases of HEV power distribution is the detection and management of the battery: in the hybrid powertrain system, the engine, the generator and the motor are controlled by the vehicle control unit (VCU) and can actively self-adjust the power load. The battery which is different to the other electric power components, delivers passive power as determined by the power difference of motors. The battery power is difficult to detect so safe limits are easily exceeded: this will affect the life and safety of the battery. So, estimating the battery state parameters especially SOC and peak power prediction is significant to battery safety operation and energy management in HEVs. Many authors have explored SOC estimation and HEV energy management. He *et al.* describe a predictive air-conditioner control system for electric buses which considers passenger amount and its variation [15]. Cao *et al.* investigated a plug-in hybrid electric bus energy management system based on stochastic model predictive control. Yang *et al.* [17] proposed a novel method of estimating the degradation and state of charge of lithium-ion batteries used for the energy management of electrical vehicles. Li *et al.* [18] proposed a novel combinatorial optimization algorithm for the energy management strategy of a plug-in HEV. Hu *et al.* [19] proposed condition monitoring for advanced battery management systems with moving horizon estimation using a reduced electrochemical model, which could be used in the battery model-based energy management of HEVs.

A PNGV(Partnership for a New Generation of Vehicles) battery model is adopted to describe the external non-linear characteristics. We consider the unscented Kalman filter method to estimate the battery SOC, and further enhance the filtering effect by the special methods of noise suppression algorithm and the invalid value elimination algorithm. Based on the UKF algorithm, this paper uses the improved UKF algorithm to estimate the SOC of the battery. Firstly, the unscented Kalman filter can estimate the battery state and suppress the influence of sampling noise during state estimation. In the second part we apply the improved noise suppression algorithm, where the Kalman filter gain and the estimated residuals are corrected to enhance the filtering effect. At the same time, the invalid value elimination algorithm is added to improve the stability of the algorithm in extreme conditions. Based on the SOC estimation and battery model, the peak power prediction method of battery is proposed and used in the power distribution strategy for Series HEV. The power distribution strategy based on battery SOC estimation and peak power prediction is tested and validated.

## II. BATTERY MODELLING AND MODEL PARAMETER IDENTIFICATION

### A. BATTERY CELL

A lithium ion battery LiFePO<sub>4</sub> has the following advantages: safe performance, no explosion in puncture testing and short-circuit testing, a long cycle life (>2,000 cycles), good performance at high temperature, wide operating temperature range and applicable in severe driving environment; large capacity, which provides a longer driving range; no memory effect, charging and discharging at any time allows vehicles to work in complicated driving conditions; light weight, reduces the weight of energy units in electric vehicles; environmental-friendly, and is free from heavy metals and rare earth metals in its production process. However, there are still some problems in its actual application, such as poor performance of charge-discharge rate, low tap density and poor performance at low temperatures.

The research object adopted a high energy 20 Ah prismatic battery, which is designed for PHEV (plug-in hybrids vehicles), EV (electric vehicles) and ReEV (Extended-Range Electric Vehicles). It behaves better in terms of charge-discharge rate, and shows improvements in low-temperature performance to a certain extent. The main performance parameters are shown in Table 1.

**TABLE 1. Main performance parameter of A123 20 Ah lithium-ion battery.**

Parameter	Value
Size ( mm )	7.25×160×227
Capacity ( Ah )	20 ( 1C , 25°C )
Nominal Voltage ( V )	3.3
Nominal Specific Power ( Wh/kg )	131
Operating Temperatures ( °C )	-30~55
Charging Capability	Continuous 20 A; transient 75 A
Internal Resistance ( mΩ )	<1.3
Mass ( g )	496
Nominal Energy ( Wh )	65
Nominal Power ( W/kg )	2400
Energy Density ( Wh/L )	247
Storage Temperature ( °C )	-40~60
Discharging Capability	Continuous 20 A; transient 100 A

### B. BATTERY MODELLING

The commonly used models of battery include electrochemical model, neural network model and lumped-parameter equivalent circuit model. Among three models the equivalent circuit model is widely used for its lower computational burden, easy parameter identification and better reflection of battery external characteristics. The lumped-parameter equivalent circuit model includes the Rint model, the first-order RC model, the high order RC model, the PNGV model, etc. According to the requirements and features of system dynamic simulation, we selected the first-order RC model, because it describes battery polarization effects better than

a Rint model and demands fewer circuit elements parameter to identify compared with other models. Thus the first-order RC model can simulate complex battery external characteristics with high precision.

The charge-discharge process of battery is a complicated electrochemical reaction processes with non-linear and time-varying properties, hence it is hard to model. The first-order RC model considers battery as a combination of a controllable voltage source, a variable resistor, and an RC structure. In addition, considering battery polarization effects, the PNGV model is adopted.

Considering the complexity of the algorithm and the accuracy of the model, PNGV battery model is adopted and displayed in Figure 1, which takes into account the characteristics of the non-linearity of the battery system.

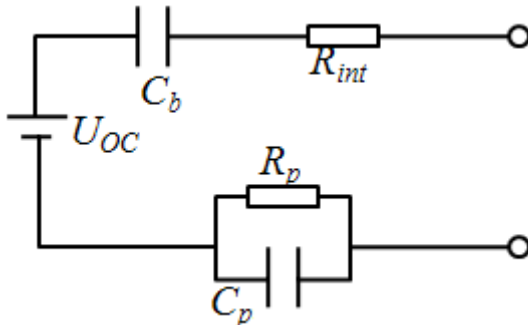


**FIGURE 1.** PNGV battery model.

The capacitor  $C_b$  in the PNGV model is used to simulate the effect of the SOC change caused by the current time integral on the open circuit voltage of the battery, which solves the problem whereby the open circuit voltage of the battery changes with the SOC. Therefore, the PNGV model can describe the battery voltage at a certain SOC of the transient response, and also can represent the steady-state response of the battery voltage.

The ideal voltage source describes the open circuit voltage of the lithium ion battery  $U_{OC}$ , and resistance  $R_{int}$  describes lithium-ion battery internal resistance. The PNGV model simulates the polarization of the battery by a resistor capacitance parallel circuit [20], and the battery capacity changes by capacitance change. The system equation for this PNGV battery model is as follows:

$$\begin{cases} U_O = U_{OC} - I R_{int} - U_P - U_b \\ \dot{U}_P = \frac{1}{C_P} I - \frac{1}{R_P C_P} U_P \\ \dot{U}_b = \frac{1}{C_b} I \end{cases} \quad (1)$$

The collecting system can acquire data about battery current and voltage: the current value is taken as an input to the system; the voltage value is the measured value thereof. The battery SOC, the capacity capacitance voltage, and the polarisation voltage are the state variables. Using the discretisation method, the state-space equation of the system can be found.

The definition of the battery SOC, based on current versus time integration, is ratio of the remaining discharge capacity and the total discharge capacity [21]. It can be calculated by the following discrete form:

$$SOC_k = SOC_{k-1} - \frac{\eta T_s}{C_n} i_k \quad (2)$$

Accordingly, the established state-space discrete equation of the battery system and measurement discrete equation are as follows:

$$\left\{ \begin{array}{l} \begin{bmatrix} SOC_k \\ u_{p,k} \\ u_{b,k} \end{bmatrix} = \begin{bmatrix} 1 & 0 & 0 \\ 0 & e^{-\frac{T_s}{\tau_p}} & 0 \\ 0 & 0 & 1 \end{bmatrix} \begin{bmatrix} SOC_{k-1} \\ u_{p,k-1} \\ u_{b,k-1} \end{bmatrix} \\ + \begin{bmatrix} -\eta T_s \\ \frac{C_n}{R_p(1 - \exp(-\frac{T_s}{\tau_p}))} \\ \frac{T_s}{C_b} \end{bmatrix} i_k \\ z_k = g(SOC_k) - u_{p,k} - u_{b,k} - i_k R_{int} \end{array} \right. \quad (3)$$

Where  $\eta = 0.98$ , denotes battery efficiency of charge and discharge,  $C_b$  denotes the battery capacity,  $g(SOC)$  denotes the functional relation between SOC of battery and open circuit voltage, obtained by the fourth-order fitting of the experimental data, which can describe the subtle changes of OCV with SOC.

### C. MODEL PARAMETER IDENTIFICATION

The battery used in the experiment was an A123 (capacity 20 Ah) and the material was lithium iron phosphate. Experimental test equipment comprised a power battery test system (10 V and 120 A, Figure 2). An HPPC(Hybrid Pulse Power Characterization) experiment which is the most commonly is used to obtain the battery equivalent circuit model parameters and the dynamic response of the battery was undertaken: the battery parameters in the battery state space equation are identified by off-line method. The least squares algorithm is used to obtain the relationship between  $R_P$ ,  $C_P$ ,  $C_b$ ,  $U_{OC}$ , and SOC. Then, the battery model is established in Simulink and the voltage of the battery model is simulated, and HPPC experimental data were compared (results shown below). As shown in Figure 2, the output voltage of the model deviates 2% at steady state and within about 5% error at outburst value compared with the experimental results.

Traditional HPPC testing entails 1 C discharge and 0.75 C charge cycling, but actually the high-power battery used in electric vehicles is supposed to work in high charge-discharge rate circumstances of up to 5 C in rapid acceleration and energy recovery working conditions, therefore polarisation effects would lead to inaccuracy in parameter estimation. Here, we set the discharge current and charge capacitance to 5 C and 3.75 C respectively, and take 10 points from 100% to 10% at 10% intervals as test points in this HPPC test.

Before the HPPC test, we emptied the battery until the battery output voltage is about 2V, which is the lower limit

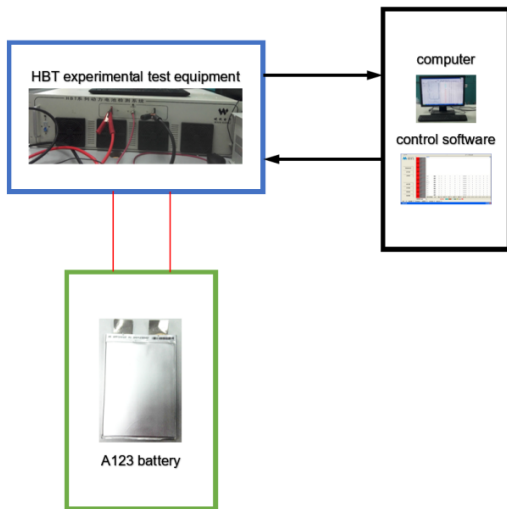


**FIGURE 2.** Battery experiment equipment platform.

available voltage of the battery. Now we considered the SOC is zero, then charge it to SOC = 1 by standard charging method. We discharge the battery in 10% power increments, carry out an HPPC test, and measure 10 points in all. The test at each point includes three steps: discharge, relaxation, and current regeneration. First discharge battery for 10 s at 5 C discharge rate (100 A), then rest for 40 s, charge battery 10 s with 75 A current. After finishing each point test, the battery was rested for one hour before continuing to avoid battery polarisation effects. The test current at each SOC point is shown in Figure 3.

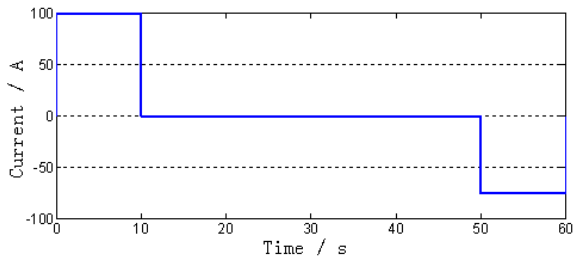


**FIGURE 3.** Hybrid Pulse Power Characterization (HPPC) Current curve in battery test.

The response data of test current and voltage, battery parameters in state space equation are identified off-line using the least squares algorithm, to obtain the relationship between  $R_p$ ,  $P$ ,  $R_{int}$ , and SOC. Then the battery model is built and simulated in Simulink, and voltage output results are compared with HPPC test data (result shown below). The output voltage error of the simulation model is less than 2%.

### III. IMPROVED UKF ESTIMATION ALGORITHM

#### A. UKF ESTIMATION ALGORITHM

The UKF algorithm is a filtering algorithm for nonlinear systems, which is fundamentally different from the EKF algorithm. It does not need to linearize the system equations, and therefore the system equation is

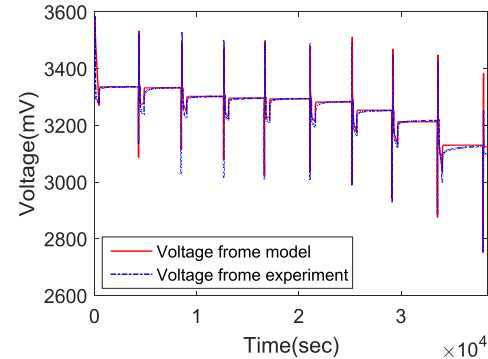


**FIGURE 4.** Comparison of battery model output with HPPC experimental data.

more accurate. The state-space equations and the measurement equations of the dynamic system are as follows [22]:

$$\begin{cases} x_k = f(x_{k-1}, u_k, w_k) \\ z_k = h(x_k, u_k, v_k) \end{cases} \quad (4)$$

The system equations and the measurement equations established above for our PNGV battery model are both non-linear and  $x_k$  denotes the state of the  $k$ th sampling period of the system, and  $z_k$  denotes the measured value, calculated by the measured equation of the state of the  $k$ th sampling period of the system. The function  $f$  denotes the state transition function, and  $h$  denotes the observation function.  $w_k$  is the system process noise, which can be regarded as Gaussian white noise with variance  $Q_k$ , and  $v_k$  is measurement noise, which can be regarded as Gaussian white noise with variance  $R_k$ .

The unscented Kalman filter algorithm is calculated as follows:

1) Determine the initial value of the state variable, and the initial covariance matrix

$$\begin{cases} \bar{x}_0 = E(x_0) \\ P_0 = E[(x_0 - \bar{x}_0)(x_0 - \bar{x}_0)^T] \end{cases} \quad (5)$$

2) Select the sigma point and calculate the mean weight and covariance weight for each sample point

$$x_{k|k}(i) = \begin{cases} \bar{x}_k, & i = 1 \\ \bar{x}_k + \sqrt{(n + \lambda)P_{k|k}}, & i = 2, \dots, n + 1 \\ \bar{x}_k - \sqrt{(n + \lambda)P_{k|k}}, & i = n + 2, \dots, 2n + 1 \end{cases} \quad (6)$$

$$w_k(i) = \begin{cases} \frac{\lambda}{n + \lambda}, & i = 1 \\ \frac{\lambda}{2(n + \lambda)}, & i \neq 1 \end{cases} \quad (7)$$

$$w_c(i) = \begin{cases} \frac{\lambda}{n + \lambda} + (1 - \alpha^2 + \beta), & i = 1 \\ \frac{\lambda}{2(n + \lambda)}, & i \neq 1 \end{cases} \quad (8)$$

Where  $n$  is the dimension of the state variable.

$\lambda = \alpha^2(n+k)-n$ ,  $\alpha \in [0,1]$  describes the distance between the sampling point and the mean point. In the normal distribution,  $\beta = 2$ , and  $k = 0$  is the ratio factor.

3) The first estimate of the system state matrix is:

$$\begin{cases} x_{k+1|k}(i) = f(x_{k|k}(i), u_{k+1}) \\ \bar{x}_{k+1|k} = \sum_{i=1}^{2n+1} W_k(i)x_{k+1|k}(i) \end{cases} \quad (9)$$

4) The first estimation of covariance of state variables matrix is:

$$P_{k+1|k} = \sum_{i=1}^{2n+1} W_c(i)(x_{k+1|k}(i) - \bar{x}_{k+1|k})(x_{k+1|k}(i) - \bar{x}_{k+1|k})^T + Q_{k+1} \quad (10)$$

5) The estimation of measured variables is given by:

$$\begin{cases} z_{k+1|k}(i) = h(x_{k|k}(i), u_{k+1}) \\ \bar{z}_{k+1|k} = \sum_{i=1}^{2n+1} W_k(i)z_{k+1|k}(i) \end{cases} \quad (11)$$

6) The estimation of the covariance of the measured variables, the covariance between the measured variables and the state variables, and the UKF gain is:

$$\begin{cases} P_{zz} = \sum_{i=1}^{2n+1} W_c(i)(z_{k+1|k}(i) - \bar{z}_{k+1|k}) \\ \times (z_{k+1|k}(i) - \bar{z}_{k+1|k})^T + R_{k+1} \\ P_{xz} = \sum_{i=1}^{2n+1} W_c(i)(x_{k+1|k}(i) - \bar{x}_{k+1|k}) \\ \times (z_{k+1|k}(i) - \bar{z}_{k+1|k})^T \\ K_{k+1} = P_{xz}P_{zz}^{-1} \end{cases} \quad (12)$$

7) The second update of the state matrix and the covariance of the state variables and return to the next iteration calculation as follows:

$$\begin{cases} x_{k+1|k+1} = \bar{x}_{k+1|k} + K_{k+1}(z_{k+1} - \bar{z}_{k+1|k}) \\ P_{k+1|k+1} = P_{k+1|k} - K_{k+1}P_{zz}K_{k+1}^T \end{cases} \quad (13)$$

## B. THE NOISE-SUPPRESSING AND INVALID VALUE-ELIMINATING ALGORITHM

The output result of our UKF algorithm is the second update of the state variables. It can be seen that the values of both real measurement and estimation of the measured variable affect the output result [23]. Due to complex and changeable factors, there is always measurement noise in the moving vehicle environment. Excessive noise can cause the algorithm to produce greater errors [24] and even divergence, which will significantly affect the accuracy. The improved estimation algorithm is designed to improve the ability of the UKF algorithm, and the correction of the measured value and the UKF gain are added to the UKF algorithm.

We calculate the estimation residuals of the measured variables and the variance of the measured variables:

$$\begin{cases} \Delta_{k+1} = |z_{k+1} - \bar{z}_{k+1|k}| \\ s_{k+1} = \sum_{i=1}^{2n+1} W_i(z_{k+1|k}(i) - \bar{z}_{k+1|k}) \\ \times (z_{k+1|k}(i) - \bar{z}_{k+1|k})^T + R_{k+1} \end{cases} \quad (14)$$

According to the basis for judging:  $\Delta_{k+1} > \sqrt{s_{k+1}}$  and using the information above, it is determined whether the current and voltage measurement are subject to interference, or not. When satisfactory, it is considered that the measured value at this time is invalid interference, and the UKF gain  $K_{k+1}$  is corrected. The correction formula is:

$$K'_{k+1} = AK_{k+1} \quad (15)$$

$A$  is defined as the correction matrix of the UKF gain.

$$A = \begin{bmatrix} \alpha_1 & & \\ & \ddots & \\ & & \alpha_n \end{bmatrix}, \quad \alpha_n \in (0, 1)$$

Especially when measurement value quietly deviates from the normal range, the filter algorithm does not update and the correction matrix is  $A = 0$ , the judgment basis is:

$$\Delta_{k+1} > \sqrt{s_{k+1}} + 200 \text{ in this condition.}$$

When the above two judgments are not satisfied, it is considered that the measured value at this time is valid, and the following judgment is adopted:  $\Delta_{k+1} > \eta s_{k+1}$ ,  $\eta \in (0, 1)$ ,  $\gamma \in (0, 1)$ . When the judgment basis is satisfied, it is considered that the error of the estimation of the measured variable at this time is large, and the estimation of the measured variable will be corrected, thus:

$$\bar{z}_{k+1|k} = \bar{z}_{k+1|k} + \beta(z_{k+1} - \bar{z}_{k+1|k}) \quad (16)$$

$B$  is defined as the correction coefficient of the estimation of the measured variable. The values of  $A$  and  $\beta$  determine the filtering effect.

All the above formulae constitute the improved UKF algorithm proposed in this work, which are used to estimate the SOC of the battery. Figure 5 shows a flow chart through the battery SOC estimation method based on the improved unscented Kalman filter algorithm.

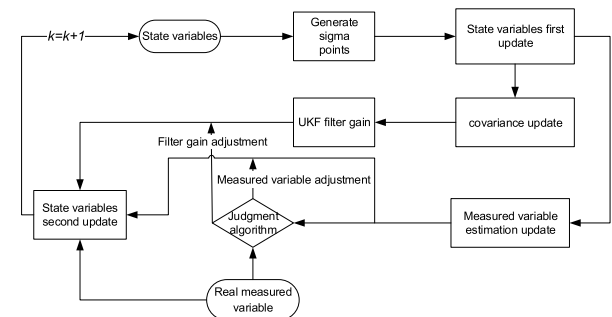


FIGURE 5. SOC estimation based on improved UKF.

## IV. HEV ENERGY MANAGEMENT STRATEGY BASED ON PEAK POWER PREDICTION OF BATTERY PACK

### A. PEAK POWER PREDICTION ALGORITHM FOR BATTERY PACK

To make full use of the power of battery pack and protect battery, further estimation of limit output power ability, including peak charge-discharge power, according to the SOC estimated by Battery Management System using the

UKF algorithm mentioned above, is required. The main aim is to estimate the maximum charge-discharge capability in the next  $\Delta t$  time based on current battery state (such as SOC), without exceeding the constraints of battery voltage, SOC, current, and power. Considering these constraints, the peak power prediction method based on voltage, current, and SOC constraints is adopted.

For the system equation of the first order RC battery model established elsewhere, when estimating the voltage in the long time to come after the input of a certain current, the amount of iterative calculations is large, and the real-time performance is poor. To estimate the discharge capacity for a long time, the transient response can be neglected and the steady state response is taken into account, now the internal resistance model can meet the demands of peak power estimation. After removing the capacitance C of the first order RC model established already, the polarisation resistance and internal resistance are connected in series to become the new internal resistance of the internal resistance model, which is used to calculate the peak power of the battery pack.

For any single cell in battery pack with series  $n_s$  and parallel  $n_p$  battery monomers, the constraints that should be satisfied are as follows:

$$\begin{cases} u_{\min} < u(k) < u_{\max} \\ z_{\min} < z(k) < z_{\max} \\ p_{\min} < p(k) < p_{\max} \\ i_{\min} < i(k) < i_{\max} \end{cases} \quad (17)$$

Where, k is the  $k$ th cell;  $u(k)$ ,  $z(k)$ ,  $p(k)$ , and  $i(k)$  are the voltage, SOC, power, current of the  $k$ th cell;  $u_{\min}$ ,  $u_{\max}$ , the minimum and maximum voltage of the cell;  $z_{\min}$ ,  $z_{\max}$ , the minimum and maximum SOC of the cell. We considered the charging as negative value and discharging as positive value, so define  $p_{\min}$  is the maximum charging power of the cell,  $p_{\max}$  is the maximum discharging power of the cell,  $i_{\min}$  is the maximum charging current of the cell, and  $i_{\max}$  is the maximum discharging current of the cell.

Considering a constraint on the voltage, the maximum discharging and charging current of the  $k$ th cell is:

$$\begin{cases} i_{\max,k}^{\text{dis,volt}} = \frac{\text{OCV}(z_k(t)) - u_{\min}}{\frac{\Delta t}{C} \frac{\partial \text{OCV}(z)}{\partial z} \Big|_{z=z_k(t)} + R_{\text{int,dis}}} \\ i_{\min,k}^{\text{chrg,volt}} = \frac{\text{OCV}(z_k(t)) - u_{\max}}{\frac{\eta_{Ah}\Delta t}{C} \frac{\partial \text{OCV}(z)}{\partial z} \Big|_{z=z_k(t)} + R_{\text{int,chrg}}} \end{cases} \quad (18)$$

Considering constraint of SOC, the maximum discharging and charging currents of the  $k$ th cell are:

$$\begin{cases} i_{\max,k}^{\text{dis,SOC}} = \frac{z_k(t) - z_{\min}}{t/C} \\ i_{\min,k}^{\text{chrg,SOC}} = \frac{z_k(t) - z_{\max}}{\eta_{Ah}t/C} \end{cases} \quad (19)$$

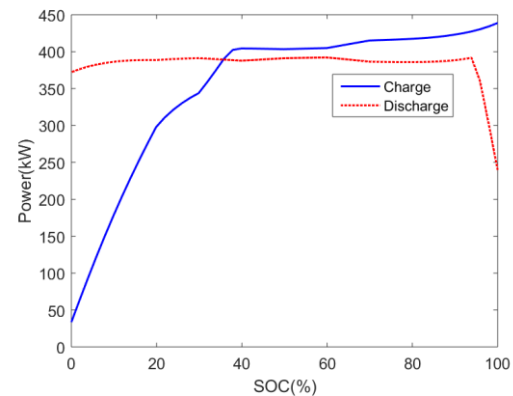


**FIGURE 6. Simulation results of peak power variation with SOC.**

The actual discharging and charging current limits of the  $k$ th cell are:

$$\begin{cases} i_{\max,k}^{\text{dis}} = \min(i_{\max,k}^{\text{dis,curr}}, i_{\max,k}^{\text{dis,SOC}}, i_{\max,k}^{\text{dis,volt}}) \\ i_{\min,k}^{\text{chrg}} = \min(i_{\min,k}^{\text{chrg,curr}}, i_{\min,k}^{\text{chrg,SOC}}, i_{\min,k}^{\text{chrg,volt}}) \end{cases} \quad (20)$$

The actual discharging and charging power limits of the  $k$ th cell are:

$$\begin{cases} P_{\max,k}^{\text{dis}} = i_{\max,k}^{\text{dis}} u_k(t + \Delta t) \\ \approx i_{\max,k}^{\text{dis}} (\text{OCV}(z_k(t)) - i_{\max,k}^{\text{dis}} \Delta t/C) - R_{\text{dis,int}} i_{\max,k}^{\text{dis}} \\ P_{\min,k}^{\text{chrg}} = i_{\min,k}^{\text{chrg}} u_k(t + \Delta t) \\ \approx i_{\min,k}^{\text{chrg}} (\text{OCV}(z_k(t)) - i_{\min,k}^{\text{chrg}} \eta_{Ah} \Delta t/C) - R_{\text{chrg,int}} i_{\min,k}^{\text{chrg}} \end{cases} \quad (21)$$

For the battery pack with series  $n_s$  and parallel  $n_p$  battery monomers, the model of the battery is based on a single battery cell model, without considering the inequality of cell group and cell work. So in this paper the peak power prediction of the battery pack is a simple multiplication of peak power of the cell and the total number of group-cells. The discharging-charging power limits of battery pack are:

$$\begin{cases} P_{\max}^{\text{dis}} = n_s n_p \min_k (P_{\max,k}^{\text{dis}}) \\ P_{\max}^{\text{dis}} = n_s n_p \min_k (P_{\max,k}^{\text{dis}}) \end{cases} \quad (22)$$

The simulation results showed that the peak charging power of battery is relatively stable, and decreases rapidly when SOC nears 100%. Moreover the peak discharging power is low when SOC is low and increases when the SOC increases. The dynamic peak power reflects the actual charge-discharge capacity of battery pack to some extent, and it is more beneficial to system safety when compared with the use of fixed calibration parameters.

## B. DESIGN OF POWER DISTRIBUTION STRATEGY BASED ON BATTERY MODEL

The coordinated power distribution of multi power sources is a core part of the integrated control strategy of hybrid power systems, and is also the prerequisite and guarantee to improving the comprehensive performance with regard to vehicle power and fuel economy. When taking power distribution strategy for series systems in which the engine-generator set

totally following the demand power of vehicle, a battery pack is used to make up for the shortage of instantaneous response from the engine-generator set, and is not involved in steady state power distribution, thus the advantages of a battery are underutilised. The battery pack can provide high discharge power in a brief time as well as giving a fast response, and also can absorb electrical power. Therefore, considering the battery pack involved in the power distribution, we decoupled the output power of the engine generator set and the power consumption of the drive motor, so that the optimal control of the engine and generator is realized. Since the demand of driving power changes in real-time and covers a wide range, the electro-mechanical power distribution based on battery model can either fully exploit the battery pack, optimize vehicle power distribution, or guarantee safety and an improved cycle life of the battery within its power limit range, also reduce the running cost of a hybrid vehicle.

The basic principle of battery pack participating in power distribution in a hybrid power system is: when the battery SOC is not in an ideal working area ( $SOC_{low} < SOC < SOC_{high}$ ), charge or discharge battery with the expected power, in order to keep the performance and energy storage of the battery pack. When battery is in an ideal working area ( $SOC_{low} < SOC < SOC_{high}$ ), arrange power for the battery pack as calculated from the optimal distribution of driving power, thus optimizing the working region of the engine for best fuel economy. When distributing power, the working ability of the battery pack and the fuel economy of the engine should be considered, so as to make the battery pack respond to the dynamic change in demand for electric power as much as possible, and make the engine work at best fuel economy.

According to the current range of battery SOC and vehicle power demands, power distribution is carried out according to the MAP diagram of engine fuel consumption rate, the minimum comprehensive fuel consumption point is selected, and the electrical power output of engine-generator set at this working point is  $P_{opt}$ . The specific power distribution rules are shown in Table 2. When the generating power arranged for engine-generator set is  $P_{opt}$ , the engine works at the minimum comprehensive fuel consumption point of fixed torque and fixed speed. When the power arranged for the engine-generator differs from this, the engine-generator set adopts the mode of multi-speed switching.

## V. EXPERIMENTAL VALIDATION AND RESULT ANALYSIS

### A. DESIGN OF EXPERIMENTAL CONDITIONS

According to the characteristics of the change of vehicle power battery load, the specific simulation conditions are designed to verify the effectiveness and anti-jamming ability of the improved UKF algorithm. Figure 7 shows the voltage signal from an experiment with sample noise.

### B. ESTIMATED RESULTS AND ACCURACY ANALYSIS

The voltage and current signals are input to the SOC estimator. The UKF algorithm and the improved UKF algorithm proposed here are used to estimate the battery SOC.

**TABLE 2. Distribution rule table for a battery participating in vehicle power distribution.**

SOC range	Power demand range	Engine-generator set power generation	Battery pack power
$SOC_{min} < SOC < SOC_{max}$	$0 < P_{need} < P_{discharge}$	0	$P_{need}$
$SOC_{min} < SOC < SOC_{max}$	$P_{charge} + P_{opt} < P_{need} < P_{discharge} + P_{opt}$	$P_{opt}$	$P_{need} - P_{opt}$
$SOC_{min} < SOC < SOC_{max}$	$P_{discharge} < P_{need} < P_{charge} + P_{opt}$ or $P_{need} > P_{discharge} + P_{opt}$	$P_{need}$	0
$SOC_{min} < SOC$ or $SOC < SOC_{max}$		$P_{need} + P_{bat}$	$-P_{bat,need}$

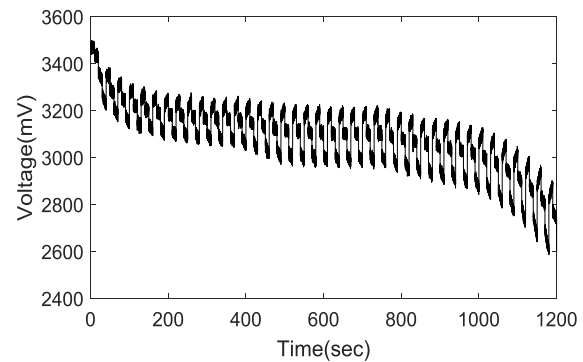


**FIGURE 7. Voltage from an experiment with sample noise.**

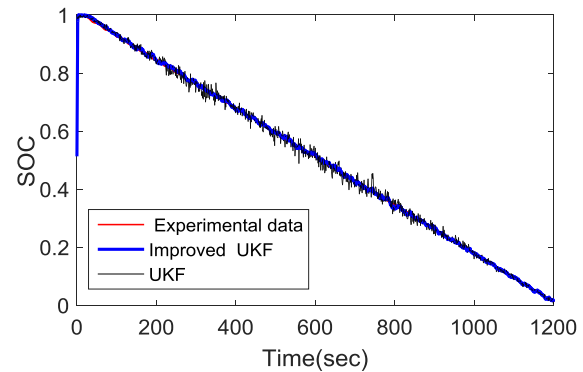


**FIGURE 8. UKF and improved UKF SOC estimation results compared with the reference SOC.**

The results (Figures 8 and 9) show that the improved UKF algorithm can significantly reduce the measurement noise estimation and SOC estimation error. The SOC estimation error is within 6%, indicating that the UKF algorithm imposed a good filtering effect on the noise signal. After further adopting the improved UKF estimation algorithm, the results show that the SOC estimation accuracy is improved, in the load conversion and under significant noise interference, the estimated error is now within 1.5%.

### C. TEST RESULTS OF POWER DISTRIBUTION STRATEGY

The test results of the power distribution strategy based on rules is shown in Figure 10, which including the vehicle speed, the fuel consumption, the speed and torque of engine

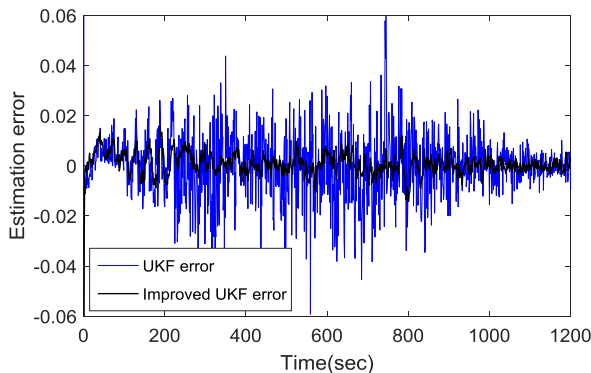


**FIGURE 9.** UKF and improved UKF SOC estimation error results.

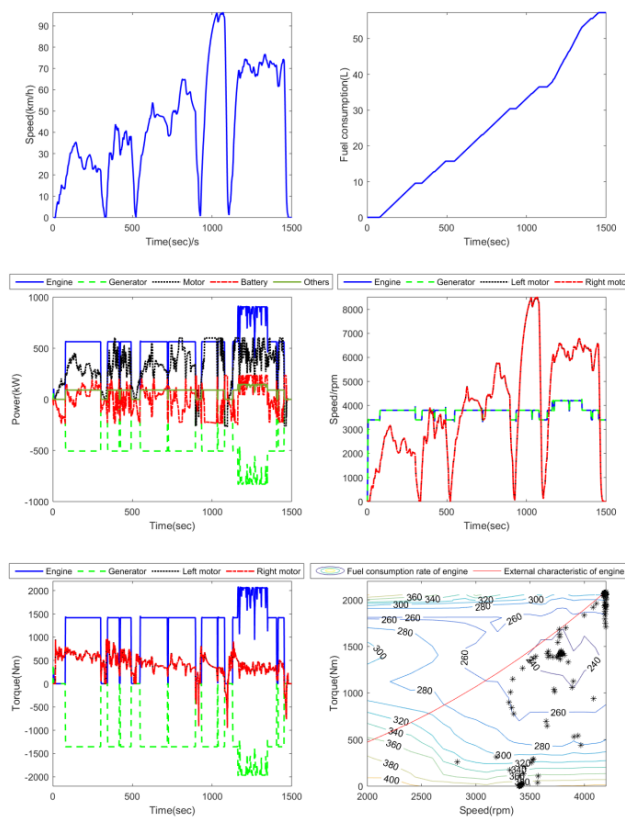


**FIGURE 10.** Simulated power distribution strategy with battery use optimization.

and motors, and so on. According to the peak power prediction of battery, in the range of its output capacity, the battery pack is involved in power distribution, so that the engine-generator set works more in high-efficiency areas, and the fuel economy of the vehicle is improved. The involvement of the battery in power distribution reduces the fuel consumption by 5%.

## VI. CONCLUSION

An improved Kalman filter algorithm is used to improve the SOC estimation of the battery. The algorithm has the advantages of moderate complexity and short computation time.

The specific condition dataset verifies that the algorithm can suppress signal noise, and has an SOC estimation error within 1.5%. Especially under significant noise interference, the improvement of the UKF algorithm remains stable, effective and accurate: the calculations are not complicated, and it offers good application prospects.

Based on the SOC estimation and battery model, the peak power prediction method of battery is proposed and used in the power distribution strategy for a Series HEV. The power distribution strategy based on battery SOC estimation and peak power prediction is tested and validated.

A rule-based power distribution strategy is developed: according to the peak power prediction of battery, in the range of its output capacity, the battery pack is involved in power distribution, so that the engine-generator set works more in high-efficiency areas, and the fuel economy of the vehicle is improved. The involvement of battery in power distribution reduces the fuel consumption by 5%.

The current research of peak power prediction in this paper focused primarily on single battery, future work will aim at the estimation considering the effect of inconsistency between cells.

## ACKNOWLEDGMENT

We thank Prof. Hongwen He and Prof. Rui Xiong in the Beijing Institute of Technology.

## REFERENCES

- [1] Y. Wang, C. Zhang, and Z. Chen, "A method for state-of-charge estimation of LiFePO<sub>4</sub> batteries at dynamic currents and temperatures using particle filter," *J. Power Sources*, vol. 279, pp. 306–311, Apr. 2015.
- [2] M. Mastali et al., "Battery state of charge estimation using Kalman filtering," *J. Power Sources*, vol. 239, pp. 294–307, Oct. 2013.
- [3] L. Y. Wang, M. P. Polis, G. G. Yin, W. Chen, Y. Fu, and C. C. Mi, "Battery cell identification and SoC estimation using string terminal voltage measurements," *IEEE Trans. Veh. Technol.*, vol. 61, no. 7, pp. 2925–2935, Sep. 2012.
- [4] Y. He, X. Liu, C. Zhang, and Z. Chen, "A new model for State-of-Charge (SOC) estimation for high-power Li-ion batteries," *Appl. Energy*, vol. 101, no. 1, pp. 808–814, 2013.
- [5] M. S. El Din, M. F. Abdel-Hafez, and A. A. Hussein, "Enhancement in Li-ion battery cell state-of-charge estimation under uncertain model statistics," *IEEE Trans. Veh. Technol.*, vol. 65, no. 6, pp. 4608–4618, Jun. 2016.
- [6] D. Andre, C. Appel, T. Soczka-Guth, and D. U. Sauer, "Advanced mathematical methods of SOC and SOH estimation for lithium-ion batteries," *J. Power Sources*, vol. 224, no. 5, pp. 20–27, 2013.
- [7] Y. Deng, Y. Hu, and Y. Cao, "An improved algorithm of SOC testing based on open-circuit voltage-ampere hour method," in *Proc. Int. Conf. Life Syst. Modeling Simulation, Int. Conf. Intell. Comput. Sustain. Energy Environ.* Berlin, Germany: Springer, 2014, pp. 258–267.
- [8] J. Chiasson and B. Vairamohan, "Estimating the state of charge of a battery," *IEEE Trans. Control Syst. Technol.*, vol. 13, no. 3, pp. 465–470, May 2005.
- [9] C. Zhang, K. Li, L. Pei, and C. Zhu, "An integrated approach for real-time model-based state-of-charge estimation of lithium-ion batteries," *J. Power Sources*, vol. 283, pp. 24–36, Jun. 2015.
- [10] M. Charkhgard and M. Farrokhi, "State-of-charge estimation for lithium-ion batteries using neural networks and EKF," *IEEE Trans. Ind. Electron.*, vol. 57, no. 12, pp. 4178–4187, Dec. 2010.
- [11] H. He, H. Qin, X. Sun, and X. Shui, "Comparison study on the battery SoC estimation with EKF and UKF algorithms," *Energies*, vol. 6, no. 10, pp. 5088–5100, 2013.

- [12] H. He, R. Xiong, X. Zhang, F. Sun, and J. Fan, "State-of-charge estimation of the lithium-ion battery using an adaptive extended Kalman filter based on an improved Thevenin model," *IEEE Trans. Veh. Technol.*, vol. 60, no. 4, pp. 1461–1469, May 2011.
- [13] C. Hu, B. D. Youn, and J. Chung, "A multiscale framework with extended Kalman filter for lithium-ion battery SOC and capacity estimation," *Appl. Energy*, vol. 92, no. 4, pp. 694–704, 2012.
- [14] Z. Chen, Y. Fu, and C. C. Mi, "State of charge estimation of lithium-ion batteries in electric drive vehicles using extended Kalman filtering," *IEEE Trans. Veh. Technol.*, vol. 62, no. 3, pp. 1020–1030, Mar. 2013.
- [15] H. He, M. Yan, and C. Sun, "Predictive air-conditioner control for electric buses with passenger amount variation forecast," *Appl. Energy*, vol. 92, pp. 694–704, 2012, doi: [10.1016/j.apenergy.2017.08.181](https://doi.org/10.1016/j.apenergy.2017.08.181).
- [16] J. Cao, J. Peng, and H. He, "Research on model prediction energy management strategy with variable horizon," *Energy Procedia*, vol. 105, pp. 3565–3570, May 2017, doi: [10.1016/j.egypro.2017.03.819](https://doi.org/10.1016/j.egypro.2017.03.819).
- [17] R. Yang, X. Rui, H. He, H. Mu, and C. Wang, "A novel method on estimating the degradation and state of charge of lithium-ion batteries used for electrical vehicles," *Appl. Energy*, vol. 207, pp. 336–345, Dec. 2017, doi: [10.1016/j.apenergy.2017.05.183](https://doi.org/10.1016/j.apenergy.2017.05.183).
- [18] L. Li, L. Zhou, and C. Yang, "A novel combinatorial optimization algorithm for energy management strategy of plug-in hybrid electric vehicle," *J. Franklin Inst.*, vol. 354, no. 15, pp. 6588–6609, 2017, doi: [10.1016/j.jfranklin.2017.08.020](https://doi.org/10.1016/j.jfranklin.2017.08.020).
- [19] X. Hu, D. Cao, and B. Egardt, "Condition monitoring in advanced battery management systems: Moving horizon estimation using a reduced electrochemical model," *IEEE/ASME Trans. Mechatronics*, vol. 23, no. 1, pp. 167–178, Feb. 2018, doi: [10.1109/TMECH.2017.2675920](https://doi.org/10.1109/TMECH.2017.2675920).
- [20] V. H. Johnson, "Battery performance models in ADVISOR," *J. Power Sources*, vol. 110, no. 2, pp. 321–329, 2002.
- [21] T. Huria, G. Ludovici, and G. Lutzemberger, "State of charge estimation of high power lithium iron phosphate cells," *J. Power Sources*, vol. 249, no. 3, pp. 92–102, 2014.
- [22] S. Abhinav and C. S. Manohar, "Bayesian parameter identification in dynamic state space models using modified measurement equations," *Int. J. Non-Linear Mech.*, vol. 71, pp. 89–103, May 2015.
- [23] Y. Wang, W. Wang, Y. Zhao, L. Yang, and W. Chen, "A fuzzy-logic power management strategy based on Markov random prediction for hybrid energy storage systems," *Energies*, vol. 9, no. 25, pp. 1–25, 2016.
- [24] X. Liu, Z. Chen, C. Zhang, and J. Wu, "A novel temperature-compensated model for power Li-ion batteries with dual-particle-filter state of charge estimation," *Appl. Energy*, vol. 123, no. 3, pp. 263–272, 2014.

**WEIDA WANG** is currently a Professor with the School of Mechanical Engineering, Beijing Institute of Technology, Beijing, China. His current research interests include hybrid vehicle, electromechanical transmission control, and energy management strategy.

**XIANTAO WANG** is currently pursuing the master's degree with the School of Mechanical Engineering, Beijing Institute of Technology, Beijing, China. He is involved in vehicle state estimation.

**CHANGLE XIANG** was the Director General with the School of Mechanical Engineering, Beijing Institute of Technology, Beijing, China, where he is currently a Professor with the School of Mechanical Engineering. He has long engaged in research in the field of vehicle's transmission and vehicle dynamics and won first and second prize of the National Prize for Progress in Science and Technology.

**CHAO WEI** is currently a Professor with the School of Mechanical Engineering, Beijing Institute of Technology, Beijing, China.

**YULONG ZHAO** is currently pursuing the Ph.D. degree with the School of Mechanical Engineering, Beijing Institute of Technology, Beijing, China. He is involved in research on energy management strategy of hybrid vehicles.

• • •